Evaluation of Piston Engine Modes and Configurations in Composite Cycle Engine Architectures

Markus Nickl
Bauhaus Luftfahrt e.V.
Junior Researcher
Willy-Messerschmitt-Str. 1, 82024 Taufkirchen, Germany
Markus.Nickl@bauhaus-luftfahrt.net

Sascha Kaiser
Bauhaus Luftfahrt e.V.
Junior Researcher

ABSTRACT

Radical aircraft propulsion concepts based on a Composite Cycle Engine architecture are presented to improve significantly the core efficiency of aero engines. Therefore, three different piston engine modes and configurations (a two-stroke and a four-stroke reciprocating piston configuration, as well as a Wankel-type rotary engine) are evaluated in order to identify the most promising piston engine concept in a Composite Cycle Engine application. The qualitative and quantitative assessment of the piston systems consider thermodynamic performance, weight and NO_x emissions, as well as cooling, lubrication and integration aspects.
To compare the performance of the different piston systems, models for the non-stationairy thermodynamic cycle of the piston engines are presented and integrated in a turbo engine performance simulation framework. A turboshaft platform with 22 MW shaft power at typical Take-Off conditions and unified state of art turbo component characteristics are used for the evaluation of the piston configurations. Further, approaches for the prediction of piston engine weights, cooling fin design and NO_x emissions are introduced.
The four-stroke reciprocation piston engine configuration is identified as most promising option due to thermal material requirements, NO_x-emissions and specific fuel consumption. It is found that the high scavenging efficiency and the lower temperature level compared to the two-stroke engine compensate the additional scavenging cycle. A preliminary geometric design of the four-stroke piston engines is illustrated for the investigated application case.

KEYWORDS: Composite Cycle, Piston Engine

NOMENCLATURE

Latin

b – cooling fin thickness
d – length
e – eccentricity
h – specific enthalpy
l – cooling fin length
m – mass
n – number of rotors
p – pressure
r – radius
s – cooling fin spacing
u – inner energy
A – surface area
H – enthalpy
P – power
Q – heat flow
R – rotor radius
T – temperature
V – volume

Greek

α – heat transfer coefficient
η – efficiency
λ – heat conductivity coefficient
ρ – density
σ – material strength
Δ – delta

Copyright © 2017 by Bauhaus Luftfahrt

1 INTRODUCTION

In order to reach aviation's long term emission reduction targets motivated by the European Commission [1] and specified by ACARE [2], significant improvements along the entire efficiency chain of the air transport system are required. Within the framework of the German national aeronautical research program (LuFo-V-2) project "Technologien für REvolutionäre ArbeitsProzesse" (TREVAP) funded by the "Bundesministerium für Wirtschaft und Energie" technologies for revolutionary thermodynamic cycle designs are investigated. One particularly promising option for significant thermal efficiency enhancement beyond the Joule-Brayton cycle engines, which is part of the TREVAP research activities, is the so-called Composite Cycle Engine (CCE). It features a piston engine in the high pressure part of a turbo engine architecture behind the intermediate pressure compressor and before the Joule combustion chamber. This allows to benefit from the partially isochoric combustion during closed volume combustion and the higher permissible peak temperatures and pressures. The CCE concept is initially discussed in [3] and [4] by Kaiser et al. and combines the high efficiency potentials of the Seiliger cycle, as present in piston engines, with the high specific power capability of gas turbine systems. In Fig. 1, the innovative thermodynamic cycle characteristics of a CCE are shown.

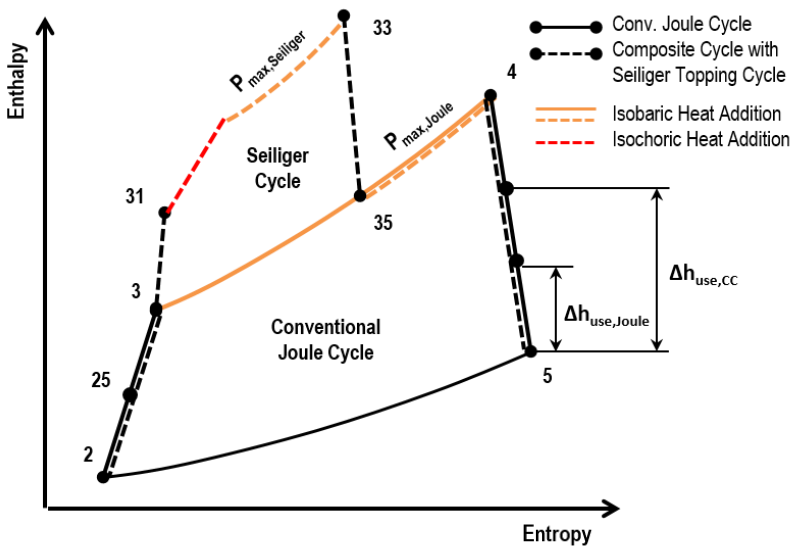

Figure 1: Enthalpy over entropy diagram of the Composite Cycle and conventional Joule-Brayton Cycle

In this paper, different piston engine concepts, in particular two- and four-stroke reciprocating piston engines as well as rotary engines as presented by Whurr [5] and Nickl et al. [6] are evaluated within a CCE architecture. Each piston engine configuration offers specific advantages, which mostly are connected with dedicated technological challenges. For example, the power-to-weight ratio of two-stroke reciprocating engines is supposed to be better than for four-stroke engines, while cooling demand and wall temperatures are more challenging due to the missing scavenging cycle. In Fig. 2, conceptual sketches of promising CCE engine architectures, which are investigated in this study, are illustrated.

In order to identify the most fuel efficient concept thermodynamic cycle studies will be presented that integrate crank angle resolved thermodynamic models of the piston engines in a turbo engine syntheses framework. The CCEs are sized to deliver 22 MW shaft output power on the low pressure spool under takeoff conditions. Beside thermodynamic efficiency, the final rating of the different piston options will also include quantitative assessments of piston system weights and NO_x-emissions as well as qualitative evaluation of technological challenges and integration aspects for each concept.

Copyright © 2017 by Bauhaus Luftfahrt

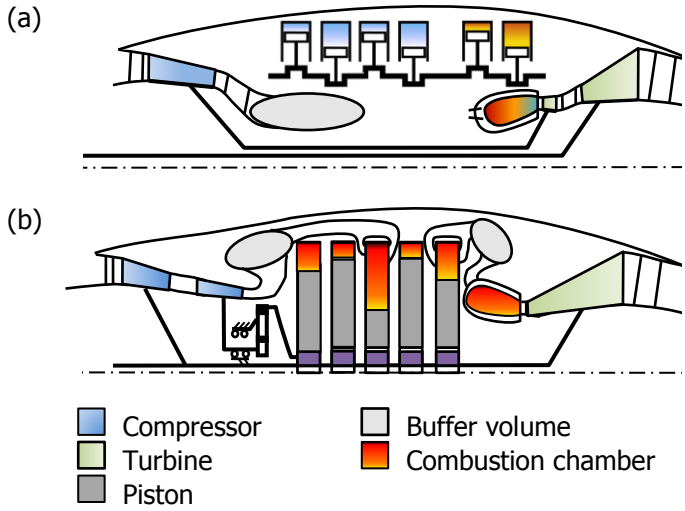

Figure 2: Basic conceptual sketches of promising CCE concepts – (a) reciprocating piston compressors and engines (2-/4-stroke), (b) rotary piston engine in coaxial arrangement

2 METHODS

For the investigation of the piston engines, parametric models are used to identify performance relevant parameters and geometric dimensions. The models provide crank angle resolved data, which can be transformed to time resolved data, to consider the non-stationary operation mode. Additionally, interactions of the piston system and the turbo engine components can be investigated by using such models. Following, the methodology of piston engine performance modelling is described in detail. Further assumptions on weight, emission and cooling demand assumptions are presented.

2.1 Thermodynamics

For piston compressor and the different piston engines, the same methodology of thermodynamic process modelling is used in principle. Differences occur during combustion and the related heat transfers. No spatial resolution of thermodynamic states in the piston volume is used, which means that cycle parameters only vary in time. For each crank angle position, chamber geometry as well as mass and energy balance are computed as illustrated in Figure 3. The cycle calculation iterates until end conditions match the starting values.

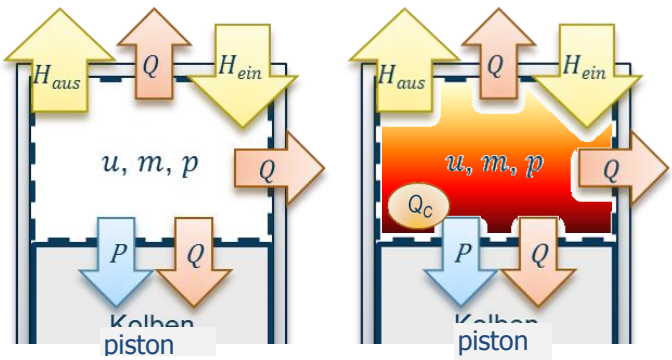

Figure 3: Schematic illustration of thermodynamic piston cycle modelling

The scavenging characteristic of the piston system during mass exchange results from inlet end exhaust valve modelling. The valves are assumed to be located at the cylinder head. Therefore, valve areas scale with piston diameter and are set to maximum feasible values for given piston diameters. For each piston, two inlet and two exhaust valves are modelled. Valve timings are defined according to crank angle with sinusoidal valve area opening and closing characteristics. Within the valve model, mass flow always develops in direction of negative pressure gradient to consider backflows through

Copyright © 2017 by Bauhaus Luftfahrt

the valves. At each crank angle position, chamber surface areas for heat transfer calculations are derived from the piston geometry. By assuming constant wall temperatures and the use of heat transfer correlations for piston engines given in [7] and [8], heat transfer from piston chamber volume to the walls are determined. The heat transfer model is illustrated in Figure 4. It considers convection at the inner piston wall, heat conduction through the wall and convection and radiation at the outer piston casing. For heat transfer at the outer wall, surrounding air flow with Mach number 0.1 and piston inlet conditions are assumed.

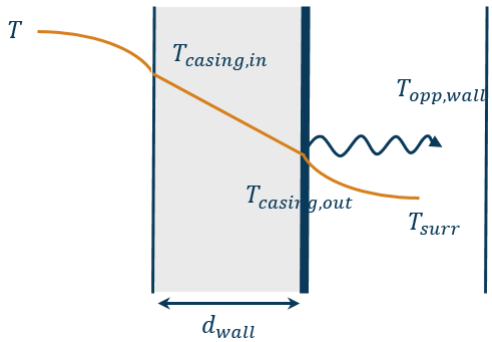

Figure 4: Schematic illustration of heat transfer modelling at the piston walls

The heat transfer model was calibrated and verified with data from NASA-CR188232 report [9]. The timeresolved rate of heat release during combustion is given by the Wiebe function [10]. Increased heat transfer as a result of enhanced turbulence due to combustion is also covered by the heat transfer correlations.

Overall thermodynamic cycle modelling and thermodynamic state parameters were also verified with NASA-CR188232 report [9]. In Figure 5, crank angle resolved piston chamber pressure are shown for the current piston model. The calculated pressure matches the reference data with minor deviations in peak pressure. In Table 1, a comparison of calculated integral cycle data with reference data is illustrated. Deviations for fuel mass, mass flow, power output heat losses and exhaust temperature are less than one percent.

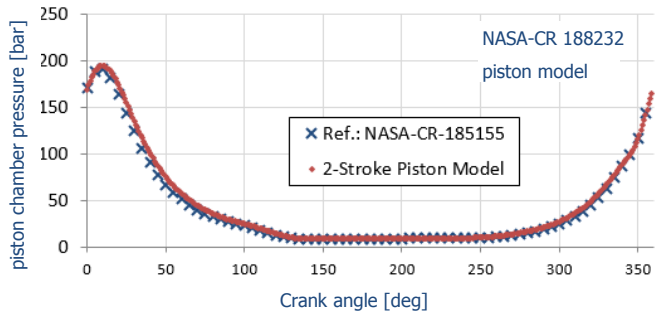

Figure 5: Verification of calculated chamber pressure of a two-stroke piston engine with reference date given in [9]

Table 1: Verification of integral piston cycle data of thermodynamic piston cycle modelling with NASA_CR 188232 reference data

Parameter	Unit	Ref.	Current	Delta [%]
Fuel	[10^{-6} kg / cycle]	49.90	49.86	-0.1
Mass flow (air)	[10^{-3} kg / cycle]	1.454	1.457	+0.2
Power output	[kW]	80.57	81.16	+0.7
Heat losses	[kW]	2.135	2.133	-0.1
Exhaust temperature	[K]	1143.0	1148.9	+0.5

Copyright © 2017 by Bauhaus Luftfahrt

The thermodynamic process modelling of the Wankel-type rotary engine follows the same principle as the described model for reciprocation piston engines. Rotary engine specific functions for chamber geometry, heat transfer [11] and valve areas are used. Additionally, leakage between rotor and casing are considered. A detailed description of the adopted rotary engine model is given in [6]. In Figure 6 important geometric parameters of Wankel-type rotary engines are depicted on the left side. At the richt side, the control volume of the rotary engine model is illustrated with the considered energy flows.

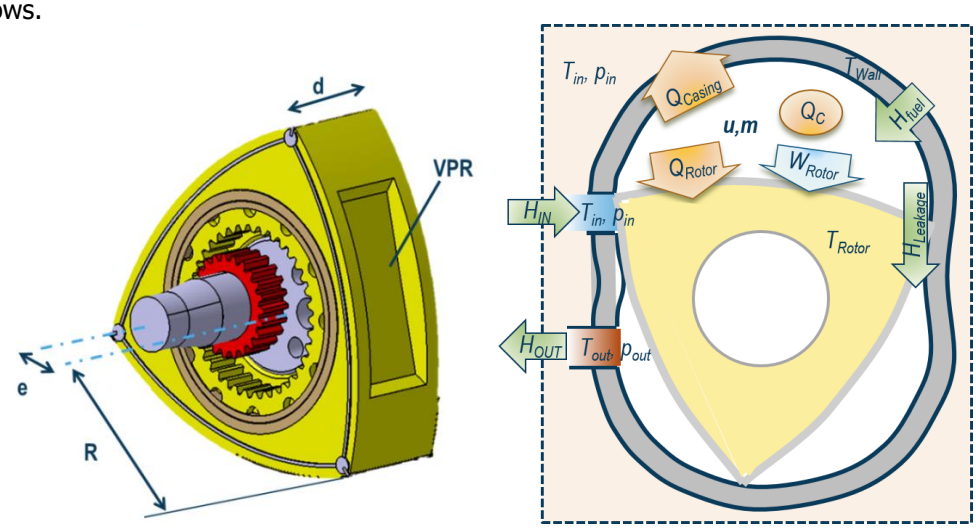

Figure 6: Rotary piston engine – left: schematic rotor illustration with main geometric parameters [6], right: control volume with considered energy flows

The crank angle resolved rotary engine performance simulation model was also verified with data from literature [11]. A comparison of calculated data (orange, "RE model") for chamber pressure, chamber temperature and heat losses for a single rotor revolution is depicted in Figure 7. A very good match of the data given in [11] is achieved. For integral performance parameters, relative errors up to 2.5 % are detected as tabulated in Table 2. These deviations result from slightly different heat transfer and valve modelling. The current model additionally considers heat input during the charging phase from the hot walls into the chamber volume and allows backflows through the valves.

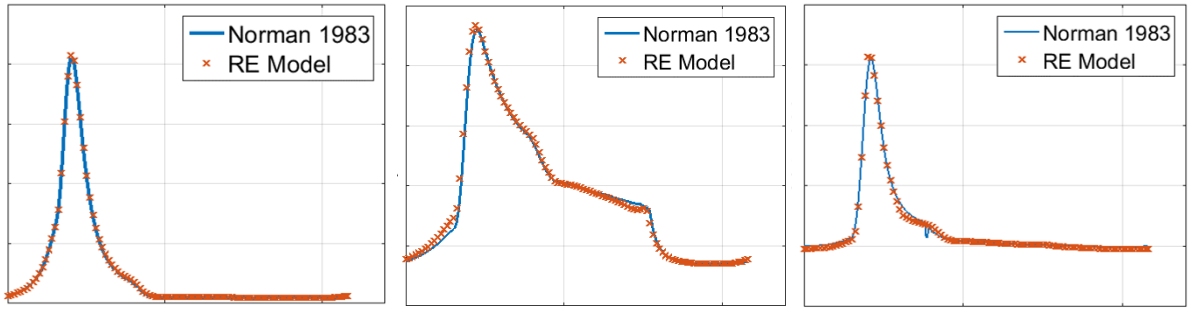

Figure 7: Verification of the thermodynamic rotary engine model – left: pressure, middle: temperature, right: heat losses, each parameter per crank angle position

Table 2: Verification rotary engine model – Comparison of important integral performance parameters

Parameter	Unit	Norman 1983 [11]	RE Model	Rel. Error [%]
Power output	[kW]	22.85	22.86	+/-0.0
Heat losses	[kW]	16.34	16.0	-2.08
Fuel	[g/s]	0.578	0.564	-2.38
Thermal efficiency	[-]	29.7	30.1	1.34
Volumetric efficiency	[-]	0.759	0.769	1.32
Max. pressure	[MPa]	4.119	4.164	+1.09

Copyright © 2017 by Bauhaus Luftfahrt

2.2 NO_x Emissions

Beside CO_2 reduction targets, the European Commission also addressed NO_x emissions within its Flightpath 2050 agenda. Therefore, the piston concepts were evaluated on NO_x emissions, too. In general, higher temperatures during combustion result in higher NO_x emissions. In piston engines, significantly higher combustion temperatures are feasible compared to conventional Joule-Brayton combustion chambers, as present in state of the art aero engines. These increased combustion temperatures are enabled by the non-stationarity of the piston cycle, which means that the high temperature arises only for a very short time during the whole piston cycle. Due to the short time of residence of the peak temperature, the chemical reaction mechanism for NO_x production does not reach chemical equilibrium at this point [21]. In consequence, less NO_x emissions compared to stationary combustion with the same peak temperature are generated.
Formation mechanism for NO_x are complex, thus a simplified correlation for NO_x emissions prediction of piston engines as presented in [12] is used. This correlation was developed for diesel piston engines with direct injection and is a lumped one step reaction model, which means that NO_x emissions are estimated from theoretical adiabatic flame temperature at the top dead centre of the piston engine. The correlation is given in Eq. (1). The adiabatic flame temperature T_{flam} is computed from combustion start temperature and the heating value of the fuel by assuming ideal stoichiometric combustion.

$$\mathrm{EINOx} = 1.6 \cdot e^{-\frac{36700\,\mathrm{K}}{T_{\mathrm{flam}}}} \qquad \textbf{(1)}$$

2.3 Weight

Introducing piston systems in turbo engine architecture will probably increase propulsion system weight, which will reduce fuel saving potential resulting from thermodynamic cycle improvement. Therefore, weight estimation for piston components is important for propulsion system evaluation of CCEs. The weight prediction model in this study uses on the one hand geometric data of the piston and piston housing, which result from thermodynamic cycle calculation. By assuming state of the art materials for piston, housing and cylinder head component weights of these parts are calculated. On the other hand, a weight breakdown, depicted in Figure 8, is used for piston engine weight estimation. The weight breakdown in Figure 8 has been taken from motors in automobile application. Due to additional components in the automotive application case, like electric generator and turbo charger, the share of "other parts" is reduced for piston engines integrated in the CCE architecture.

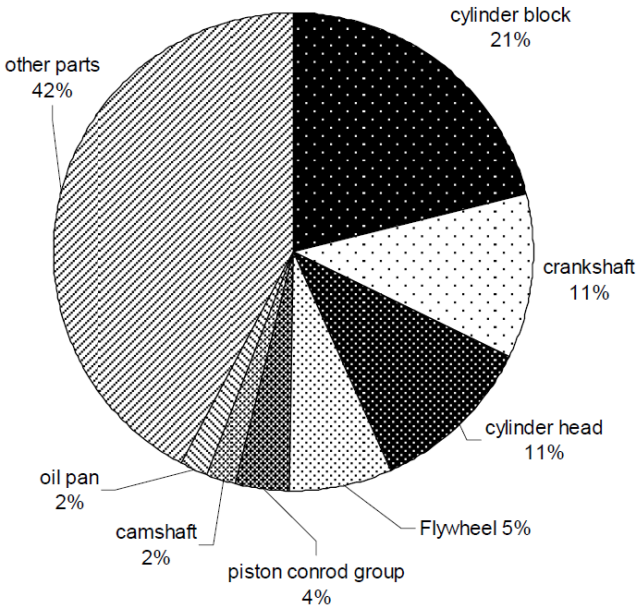

Figure 8: Percentage weight brakedown for piston engine components [13]

Copyright © 2017 by Bauhaus Luftfahrt

For weight prediction of rotary engines, a correlation published in NASA-TM-X71906 [14] is used. With this correlation rotor and casing weight (Eq. (2) and (3)) is determined by the use of main geometric parameters like rotor radius R, eccentricity e and the number of rotors n, the casing material properties σ (strength) and ρ (density) and the cycle peak pressure p_{cl}. Again, these geometric data result from thermodynamic cycle calculation. The weight of cooling fins and other components are considered by calibration factors, leading to the total rotary engine weight as shown in Eq. (4).

$$m_{\text{casing}} = \frac{\pi R^2 (1 + (e/R))^2 p_{cl}}{\sigma/\rho} [\frac{2}{3} \cdot nR + (n+1)R(1 + (\frac{e}{R}))] \quad \textbf{(2)}$$

$$m_{\text{rotor}} = 0.5 \cdot V_{\text{rotor}} \cdot \rho_{\text{rotor}} \quad \textbf{(3)}$$

$$m_{\text{total}} = 1.18 \cdot (1.5 \cdot m_{\text{casing}} + m_{\text{rotor}}) \quad \textbf{(4)}$$

2.4 Cooling fin layout

The heat losses of the piston engine resulting from thermodynamic cycle calculation is assumed to be rejected by an air cooling system. Therefore, cooling fins were provided, to increase the feasible heat transfer at the outer piston casing. A simplified approach for cooling fin design is used to get a rough estimation of the necessary volume and weight. Hence, a rectangular cooling fin profile is assumed. Figure 9 shows a section of the piston engine cylinder with a detailed zoom on the cooling fins, where main geometric parameters of the fins are illustrated.

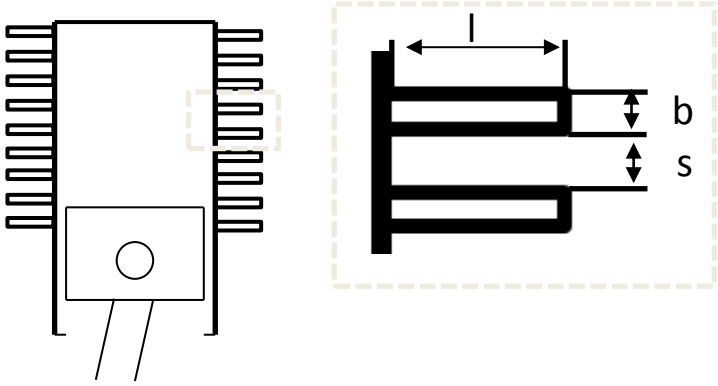

Figure 9: Cooling fin design for piston engine

A share of the main core mass flow, which is not lead through the piston cylinder, is used as cooling fluid. Fluid velocity is set to Mach 0.1. For these conditions, rejectable heat is calculated by Eq. (5), as published in [15]

$$Q_c = \alpha_{\text{sum}} \cdot (T_{\text{w}} - T_{\text{cool}}) \cdot A_0 \cdot [(2l + s)/(b + s)] \cdot \eta_c \quad \textbf{(5)}$$

In Eq. (5) surface area of the cylinder without cooling fins is named with A_0 and cooling fin efficiency with η_c. For volumetric optimized cooling fins, which are in first approximation also weight optimal, this efficiency equals 0.627 [16] in case of rectangular cooling fin profiles. T_w and T_{cool} describe the involved temperatures of the wall and the surrounding cooling fluid. The heat transfer coefficient α_{sum} considers heat conduction from the cooling fin root and convective heat transfer into the fluid. It is calculated by

$$\alpha_{sum} = \left(\frac{r_o \ln\left(\frac{r_o}{r_i}\right)}{\lambda} + \alpha^{-1} \right)^{-1}, \quad \textbf{(6)}$$

using the cooling fin root (r_i) and tip diameter (r_o) as well as the heat conductivity coefficient λ of the cooling fins and the convective heat transfer coefficient α. For the piston engine, presented later on, 13 cooling fins with depth b = 5 mm, vertical spacing s = 10 mm and a fin length of l = 50 mm the heat losses resulting from thermodynamic cycle calculation can be rejected. The resulting weight of the cooling fins is 20.9 kg per cylinder.

Copyright © 2017 by Bauhaus Luftfahrt

2.5 Integration in Aircraft Propulsion System Synthesis

For evaluation of the piston systems in a CCE architecture, the previously described performance models are integrated into the Bauhaus Luftfahrt in-house Aircraft Propulsion System Syntheses (APSS) framework. In APSS, a component based, modular representation of the turbo engine architecture is used for power plant performance calculation. During cycle calculation iterations, common sizing and design heuristics reported in [17,18] are applied. Following the flow path through the engine, changes in thermodynamic state variables are computed. The power request from the piston engine is given by the mechanically connected compressors. With fluid input conditions according to compressor outlet and a technologically limited maximum peak pressure in the piston engine cycle, piston systems and geometries, which are able to fulfill the performance requirements, are derived.

3 RESULTS

Following, results from a qualitative concept analysis and piston system data calculated with the previous introduced models are presented. For the most promising concept, a detailed design of the piston components will be shown. Typical take-off conditions are used for propulsion system comparison and component sizing point.

3.1 Evaluation of piston concepts

The qualitative assessment of the piston engine concepts is based on typical characteristics of the three investigated piston systems as known in literature [19, 20] and independent from the TREVAP application case. The piston systems are evaluated on thermal and volumetric efficiency, power to weight ratio, thermal stresses and aspects of lubrication, sealing and cycle characteristics. On the one hand, the two-stroke engine offers a good power to weight ratio with small integration volume. On the other hand, low volumetric efficiency due to poor scavenging behavior and challenging thermal stresses due to burning in every revolution are connected with the two-stroke piston system. On the contrary, the four-stroke engine offers very high volumetric efficiency to the cost of higher complexity and more discrete power delivery. Further, better lubrication is achievable for this engine. The rotary engine offers best power to weight ratio and can be integrated coaxially to the turbo components. But sealing between the single chambers is very challenging and complex, less efficient sealing systems are in use. Additionally, lubrication of the rotor is very difficult. A significant share of the lubricant is burnt during the cycle.
For quantitative evaluation of the different piston systems, integrated thermodynamic cycle calculations on propulsion system level are computed. Therefore the project specific application case of 22 MW shaft power on the low pressure spool and 1.1 MW residual core flow power under typical take-off conditions (Mach number 0.25, sea level, ISA+15) are used. The chosen conditions represent the relevant sizing point for piston engine and secondary air system, but do not indicate full fuel saving potential of CCE's in typical cruise conditions, as presented in previous assessments of integrated CCE performance [3]. Thermodynamic cycle calculation of the piston systems is operated with the previously described models. For all piston concepts, cycle peak pressure is set to 25 MPa. Table 3 lists important results from these calculations. Compared to state of the art turbo engines, thermal efficiency of the CCE concepts improves between 7.9 % (rotary engine) and 8.5 % (four-stroke engine) for the investigated conditions. In case of the two-stroke engine, results from qualitative assessment are confirmed. High wall temperatures and poor volumetric efficiency are observed. It is found, that in case of the four-stroke engine, high volumetric efficiency and lower temperature level during the charging phase compensate for the half power output rate, leading to very similar piston diameters (assuming same number of pistons for the two- and the four-stroke engine). Due to the lower cycle temperature level, less NO_x emissions are predicted for this piston mode. The rotary engine offers a substantial weight saving potential. For comparability reasons, peak pressure of 25 MPa was assumed here, too. However, this pressure level is not achieved by state of the art rotary engines. Dimensions and weight saving potential become rapidly worse by assuming lower peak pressures. Therefore, the four-stroke reciprocating piston system is chosen as best option. Following, a detailed design of a four stoke piston engine for the TREVAP application case is presented.

Copyright © 2017 by Bauhaus Luftfahrt

Table 3: Characteristic cycle data for different piston engine configurations

Parameter	Unit	2-stroke engine	4- stroke engine	Rotary engine
Wall temperature	[K]	1212	1005	884.5
Heat losses	[kW]	572.7	320.9	1010
Fuel consumption	[kg/s]	0.533	0.532	0.589
Peak pressure	[MPa]	25.00	25.00	25.00
Weight	[kg]	1916	1914	1369
Volumetric efficiency	[-]	0.491	0.967	0.980
Exhaust temperature	[K]	1078	1089	1113
Total efficiency	[-]	0.367	0.367	0.342
Piston diameter	[m]	0.227	0.226	~0.9
Number of pistons	[-]	15	15	5
NO_x-emissions	[g_{NOx}/kg_{fuel}]	172	148	125

3.2 Piston system design

For the preferred four-stroke piston engine a preliminary geometric design is derived from the thermodynamic cycle calculations and the resulting performance requirements. Therefore, three piston engines in V-arrangement around the turbo engine shaft are assumed. Each piston engine consists of eight piston compressors and six lighted pistons. In total, 24 piston compressor and 18 piston engine cylinders are used. The relevant geometric data of the piston components are listed in Table 3. The piston engine cylinders have smaller inner diameters, due to cooling fins at the outer cylinder surface. All cylinders are supposed to have a stroke of 0.15 m. The piston compressors operate with a geometric compression ratio of 24 and deliver a pressure ratio of 3.92. For the piston engine, a compression ratio of 10.3 is used. The buffering volumes in front of the piston compressor and after the piston engine are sized to reduce the total pressure fluctuation at the connected turbo components to less than 1 % of the corresponding mean pressure level. In Fig. 10, a possible basic arrangement of the piston components in the Composite Cycle Engine architecture is illustrated. A longitudinal and a transversal section of the engine is shown. Additionally, one piston compressor cylinder and one piston engine cylinder are depicted in detail with most important dimension data.

Table 4: Piston engine component data

Parameter	Unit	Piston Compressor	Piston Engine
Number of pistons	[-]	24	18
Inner piston diameter	[m]	0.273	0.195
Stroke	[m]	0.15	0.15
Cylinder casing length	[m]	0.30	0.30
Total displacement volume	[m^3]	0.211	0.080
Compression ratio	[-]	24.0	10.3
Pressure ratio (p_{out}/p_{in})	[-]	3.92	1.0
Buffer volume	[m^3]	0.023	0.063

Parameter	Unit	Piston Engine
Rotation speed	[rpm]	3000
Length (axial)	[m]	~2.1
Outer diameter	[m]	~1.6
Inner diameter	[m]	~1.0

Copyright © 2017 by Bauhaus Luftfahrt

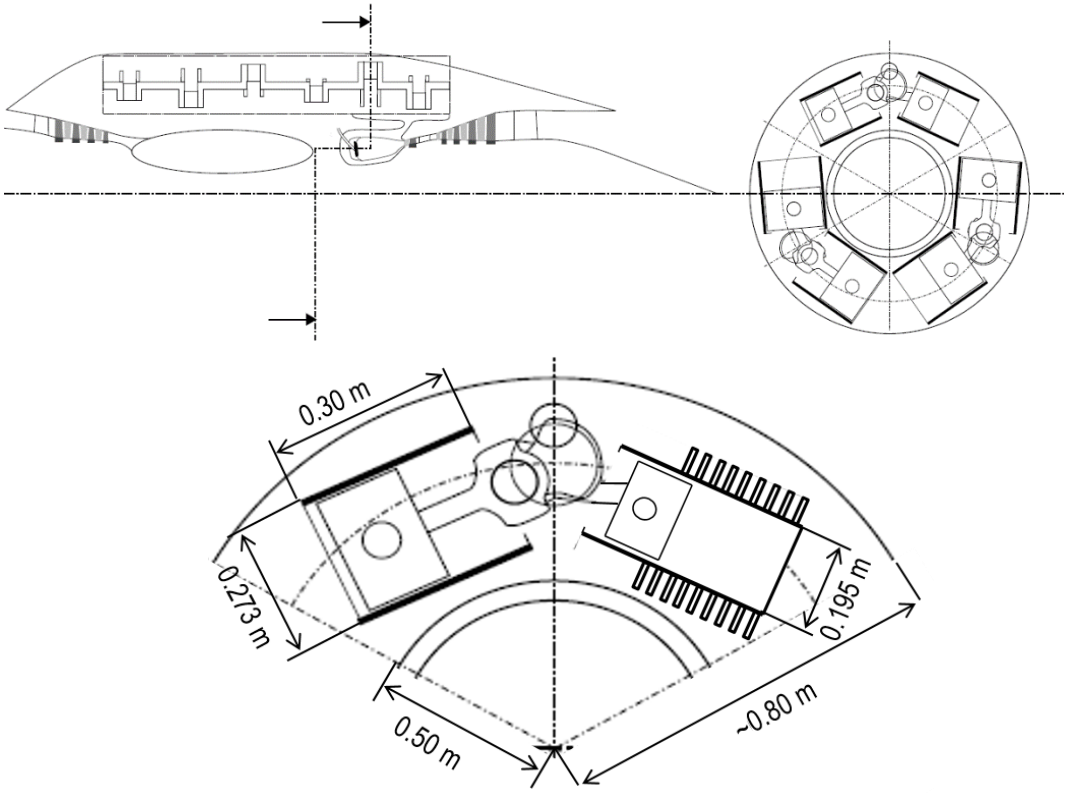

Figure 10: Illustration of piston engine integration and geometry (modified from [3])

4 CONCLUSION

In the present paper, three different piston engine systems are evaluated in a CCE architecture for the TREVAP project specific application case of a 22 MW turbo shaft engine at typical take-off conditions. In case of the conceptually promising coaxial arranged Wankel-type rotary engine, technological challenges concerning the peak pressure level and the chamber sealing, especially at the rotor tips, are identified which might not be sufficiently solved in the near future. Shortfalls in these issues significantly worsen the thermodynamic performance. Therefore, the rotary engine concept is not viable until further technological advancements will have been achieved.
Compared to the rotary engine configuration, the reciprocating piston systems are less challenging in terms of technological requirements. For the two-stroke piston configuration, the expectation of a higher power to weight ratio compared to the four-stroke mode is disproved during the quantitative cycle evaluation. The poor scavenging efficiency and the higher temperature level of the two-stroke engine cycle lead to a similar needed cylinder diameter for both concepts, while assuming the same number of pistons. In consequence, the four-stroke piston mode outperforms the two-stroke piston system due to less heat losses and lower NO_x emissions. The lower wall temperatures also decrease thermal load of the piston material, enabling the use of lighter materials.
A preliminary design of the selected four-stroke piston configuration consists of three piston engines in a V-arrangement around the turbo engine core with 24 piston compressors and 18 piston engine cylinders in total. All cylinders are designed to have similar outer diameters of approximately 0.3 m. While cooling fins are needed to reject the heat from the lighted cylinders, the inner diameter of the piston engine cylinders is reduced to 0.195 m.

Copyright © 2017 by Bauhaus Luftfahrt

REFERENCES

[1] European Commission; 2011; "Flight-Path 2050: Europe's Vision for Aviation"; Publications Office of the European Union; Luxembourg.
[2] ACARE; 2012; "Strategic Research & Innovation Agenda - Volume 1".
[3] S. Kaiser et al.; 2016; "A Composite Cycle Engine Concept with Hecto-Pressure Ratio"; *Journal of Propulsion and Power*; **32**(6); doi: 10.2514/1.B35976
[4] S. Kaiser et al.; 2016; "Unified Thermodynamic Evaluation of Radical Aero Engine Cycles"; *ASME Turbo Expo*; Seoul; June 26-30.
[5] J. Whurr; 1997; "Aircraft Compound Cycle Propulsion Engine"; United States; US5692372.
[6] M. Nickl, S Kaiser, A Seitz, M. Hornung; 2016; "Performance Modeling of a Composite Cycle Engine with Rotary Internal Combustion Engine"; *Deutscher Luft- und Raumfahrt Kongress*; **65**; Braunschweig; September 13-15; ID 420144.
[7] G. Woschni; 1968; "A Universally Applicable Equation for the Instantaneous Heat Transfer Coefficient in the Internal Combustion Engine"; *SAE Transactions*; **76**, paper 670931.
[8] G. Hohenberg; 1980; "Experimentelle Erfassung der Wandwärme von Kolbenmotoren"; *Habilitation*; TU Graz.
[9] J. Van Gerpen; 1990; "Simulation of a Combined-Cycle Engine"; NASA Contractor Report 188232; Iowa State University.
[10] I. Wiebe; 1970; "*Brennverlauf und Kreisprozess von Verbrennungsmotoren*"; VEB Verlag Technik; Berlin.
[11] T.J. Norman; 1983; "A Performance Model of a Spark Ignition Wankel Engine Including the Effects of Crevice Volumes, Gas Leakage and Heat Transfer"; *Mechanical Engineering Master-Theses*; Massachusetts Institute of Technology.
[12] P.Andersson; 1989;"Model for predicting the NOx exhaust pollutants in a diesel engine"; *Master Theses*; Lund.
[13] M. Cagri Cevik et al; 2009; "Cranktrain Design Optimized for Reducing Weight and Friction Supported by Coupled CAE Tools"; *Technical Report*; FEV Motorentechnik GmbH; Aachen.
[14] K.C. Civinskas, G.A. Kraft; 1976; "Preliminary Evaluation of a Turbine/Rotary Combustion Compound Engine for a Subsonic Transport Aircraft"; *NASA Technical Memorandum TM X-71906*; U.S. Army Air Mobility R&D Laboratory; Cleveland, Ohio.
[15] Mollenhauer K. Tschöke H. „Handbuch Dieselmotoren", Springer-Verlag Berlin, 2007.
[16] W. Polifke, J. Kopitz; 2009; "*Wärmeübertragung – Grundlagen, analytische und numerische Methoden*"; 2nd Edition; Pearson-Verlag; Hallbergmoos.
[17] A. Seitz; 2012; „*Advanced Methods for Propulsion System Integration in Aircraft Conceptual Design*"; Dissertation; Technical University Munich.
[18] H. Grieb; 2004; "*Projektierung von Turboflugtriebwerken*"; Birkhäuser Verlag; Basel-Boston-Berlin.
[19] R. Van Basshuysen; 2010; „*Handbuch Verbrennungsmotoren*"; 5th Edition; Vieweg+Teubner Verlag Wiesbaden.
[20] Kraemer, Jungbluth; 1983; „Bau und Berechnung von Verbrennungsmotoren", 5th Edition, Springer-Verlag Berlin.
[21] C.D. Rakopoulos, et al; 2003; „Development and validation of a comprehensive two-zone model for combustion and emissions formation in a DI diesel engine"; *International Journal of Energy Research*; **27**; pp 1221-1249; doi: 10.1002/er.939

Copyright © 2017 by Bauhaus Luftfahrt